

# *Neural systems involved in spatial discrimination based on viewer- and object-centered reference frames; A study using the LORETA analysis of event-related potentials*

*Yuriko Kiriya<sup>1-4</sup>, Katsumi Umeno<sup>1-3</sup>, Etsuro Hori<sup>1-3</sup>, Yang Li<sup>1,2</sup>, Nobuyuki Sunahara<sup>4</sup>, Taketoshi Ono<sup>1-3</sup>, Hisao Nishijo<sup>1-3</sup>*

---

## ABSTRACT

Event-related potentials (ERPs) were recorded while the subjects detected defective parts of circles, presented on a monitor, based on the viewer- and object-centered reference frames. These figures elicited the ERPs mainly at the parietal areas. A sLORETA analysis of the ERPs indicated that current source density (CSD) was higher at the dominant right parietal lobe in the both tasks based on the viewer- and object-centered reference frames. Furthermore, CSD was higher at the superior frontal and superior temporal gyri only in the object-centered reference frame task. The results, along with the previous anatomical data, suggest an involvement of the dorsal visual pathways in the viewer-centered reference frame while the both dorsal and ventral visual pathways might be involved in the object-centered reference frame. These results further suggest that the both visual pathways might converge on the right dominant parietal lobe.

**Key words:** Spatial hemineglect, spatial discrimination task, event-related potentials, current source density, parietal lobe.

---

<sup>1</sup>System Emotional Science, Graduate School of Medicine and Pharmaceutical Sciences, University of Toyama

<sup>2</sup>CREST, JST.

<sup>3</sup>JSPS Asian Core Program

<sup>4</sup>Toyama Prefectural Koshi Rehabilitation Hospital

Correspondence to: Dr. H. Nishijo.  
System Emotional Science  
Graduate School of Medicine and Pharmaceutical Sciences  
University of Toyama  
Sugitani 2630, Toyama 930-0194, Japan  
Tel.: +81-76-434-7215; Fax: +81-76-434-5012  
E-mail: [nishijo@med.u-toyama.ac.jp](mailto:nishijo@med.u-toyama.ac.jp)

## INTRODUCTION

Spatial hemineglect refers to the defective ability of patients with unilateral brain damage to explore the side of space contralateral to the lesion (contralesional), and to report stimuli presented in that portion of space (Vallar, 1998). A left neglect syndrome is most commonly observed in right brain-damaged patients and is often dramatic enough to constitute a major handicap (Heilman and Valenstein, 1979; Vallar, 1993). The left spatial hemineglect usually occurs after injuries of the middle cerebral artery (Heilman et al., 1983; Vallar and Perani, 1986; Leibovitch et al., 1998; Vallar, 2001) or posterior cerebral artery (Cals et al., 2002). Its responsible lesions have been debated; the right parietal lobe, right side of the right temporo-occipital junctional region, superior temporal gyrus, or right frontal lobe, etc., which vary according to the reports (Heilman et al., 1983; Vallar and Perani, 1986; Leibovitch et al., 1998; Mesulam, 1999; Vallar, 2001; Karnath et al., 2004). Various neural mechanisms of spatial hemineglect have been proposed based on its symptoms; sensory inattention (Brain, 1941), eye movement disorder (Malhotra et al., 2006), impairment of reciprocal inter-hemispheric inhibition (Kinsbourne, 1977; Hilgetag et al., 2001), unilateral arousal disorder (Mesulam, 1982; Heilman et al., 1985), unilateral hypokinesia (Heilman and Valenstein, 1979), contralesional loss of representational space (Bisiach and Luzzatti, 1978; Bisiach et al., 1996), and transection of the cerebral white matter fiber (Baltoromeo et al., 2007).

The above inconsistent results suggest that neglect is a heterogeneous condition. Indeed, the detailed analysis of these studies has demonstrated that there are two kinds of cases of spatial neglect; an impairment of attention to objects presented in the contralesional side of space relative to the head, body, or visual field (viewer-centered neglect), and an impairment of attention to the contralesional side of an individual object regardless of its location with respect to the viewer (stimulus-centered neglect) (Ota et al., 2001, 2003). These 2 types of neglect are

comparable to egocentric and allocentric neglect, respectively (Chatterjee, 1994; Hillis et al., 2005; Marsh and Hillis, 2008). These results suggest presence of at least 2 different reference frames that represent external environmental information in the brain, and that the differences among the symptoms are attributed to differences of the impaired reference frames (Myers, 1999). One of the 2 reference frames is a viewer-centered reference frame, and the other, an object or stimulus-centered reference frame (allocentric reference frame) (Hillis, 2006). In the viewer-centered reference frame, the origin of space coordinate axes is located at the center of the visual field (or the center of the head or body of the viewer), while the origin is located at the center of the object in the stimulus-centered reference frame.

A recent neurological study using patients with brain damages suggested that the right angular gyrus (right inferior parietal lobule) was responsible for neglect to the left side of patients (egocentric neglect), while the right superior temporal gyrus was responsible for neglect to the left side of objects (allocentric neglect) (Hillis et al., 2005). A functional MRI study using healthy subjects suggested that the superior parietal lobule was associated with the viewer-centered reference frame, while the superior temporal gyrus is associated with the object-centered reference frame (Neggers, 2006). A neurophysiological study using monkeys reported that neurons in the frontal eye field responded to stimuli in the object-centered reference frame (Olson, 2003). These studies suggest that at least 2 different neural systems for the 2 different reference frames might function. However, it remains unknown precise time course of activity of the above various brain regions in spatial discrimination tasks based on the 2 different reference frames.

In the present study, to analyze temporal changes in activity in these brain regions, event-related potentials (ERPs) were recorded in spatial discrimination tasks based on the viewer-centered and object-centered reference frames. The current source density of ERP components was analyzed by the standardized low-resolution brain electromagnetic tomography (sLORETA) method (Pascual-Marqui, 2002).

## METHODS

### 1) Subjects

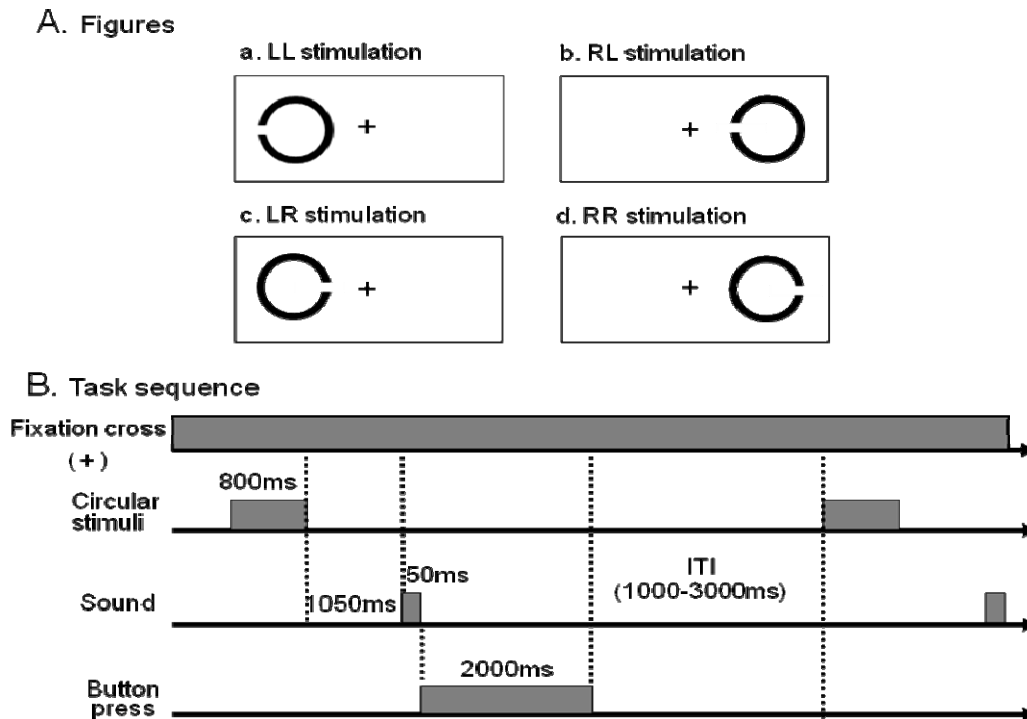
Five healthy subjects were enrolled (mean age  $32 \pm 2.6$  yrs; range, 24 to 39 yrs; 3 females, 2 males; 4 right-, and 1-left handed). All subjects were treated in strict compliance with the Declaration of Helsinki and U.S. Code of Federal Regulations for protection of human subjects. The experiments were conducted with the understanding and consent of each subject, and approved by the ethical committee at our university.

### 2) Spatial discrimination tasks

In the present study, four kinds of the figures (circles) were presented according to the study by Ota et al. (2003) (Fig. 1A). The circles with an external diameter of 3 cm, either end of the sides of which was defective, were displayed at 8 cm left or 8 cm right from the center (indicated by "+" mark) of the monitor. These four kinds of the circles were based on the defective areas and position of the circles on the monitor: 1) the circle was presented at the left of the monitor and the left side of the circle was defective (LL stimulation), 2) the circle was presented at the right of the monitor and the left side of the circle was defective (RL stimulation), 3) the circle was presented at the left side of the monitor and the right side of the circle was defective (LR stimulation), and 4) the circle

was presented at the right of the monitor and the right side of the circle was defective (RR stimulation). Thus, the circles look like "C" or "reversed C".

Two discrimination tasks were performed in random order. In the viewer-centered reference frame (VCT) task, the subjects were required to identify whether stimulation figures were on the right or left of the "+" mark, located at the center of the monitor, while they were required to identify whether a defective part of a circle was at the left or right end of the circle in the object-centered reference frame (OCT) task. In the both tasks, the "+" mark was always displayed at the center of the monitor and the subjects were asked to fixate it. In both of the tasks, four kinds of stimulation figures (LL, RL, LR and RR) were randomly displayed for 800 msec (Fig. 1B). A signal sound (50 msec) was generated 1050 msec after the disappearance of stimulation, and the subjects were required to press a key on a keyboard within 2000 msec after the sound. When the subjects judged the position of the defective part to be to the left, they required to press a left directional operation key ( $\leftarrow$ ), and to presse a right directional operation key ( $\rightarrow$ ) when they judged it to be to the right. The inter-task interval between trials was randomly set at 1000 to 3000 msec and each of the tasks was performed for 22 to 24 min.



**Fig. 1.** Schematic representation of the stimulus presentation in the viewer-centered (VCT) and object-centered (OCT) tasks.

**A:** Visual stimuli. a, a circle whose left side end was missing was presented to the left side of the center ("+" mark) of the monitor (LL stimulation). b, a circle whose left side end was missing was presented to the right side of the center ("+" mark) of the monitor (RL stimulation). c, a circle whose right side end was missing was presented to the left side of the center ("+" mark) of the monitor (LR stimulation). d, a circle whose right side end was defective was presented to the right side of the center ("+" mark) of the monitor (RR).

**B:** Time course of the tasks. Fixation cross "+" was always presented at the center of the monitor, and the subjects were instructed to fixate it. The figures were presented in random interval. After the figures disappeared, a signal sound was presented and the subjects were required to press a key on the keyboard.

## 2) Recording and analyses of electroencephalograms (EEGs)

According to the International 10-20 system, 60 EEG electrodes were placed on the scalp. The EEGs were continuously recorded using a 128ch amplifier (Nihon Kohden, EEG-1100). These were referred to the tip of the nose, and the impedance was kept below 5 K $\Omega$ . A ground electrode was placed on the forehead. The EEGs were filtered (0.3 to 120 Hz) and digitized (sampling rate, 500 Hz). The electrooculograms (EOGs) were also recorded to detect eye blinking and movements.

In EEG analyses, various noises including EOGs were removed using the independent component analysis (ICA). Then, the EEG data were segmented between -200 to 800 msec in reference to the onset of visual stimuli, and visual evoked potentials (VEPs) were summed and averaged in individual channels for each of four circles in the VCT

and OCD tasks. Finally, the grand averaged ERPs were computed across the subjects. Electric potential distribution of ERP was converted into the current source density (CSD) topography to analyze the input and output current distribution across the scalp using EEGLAB (Delorme and Makeig, 2004).

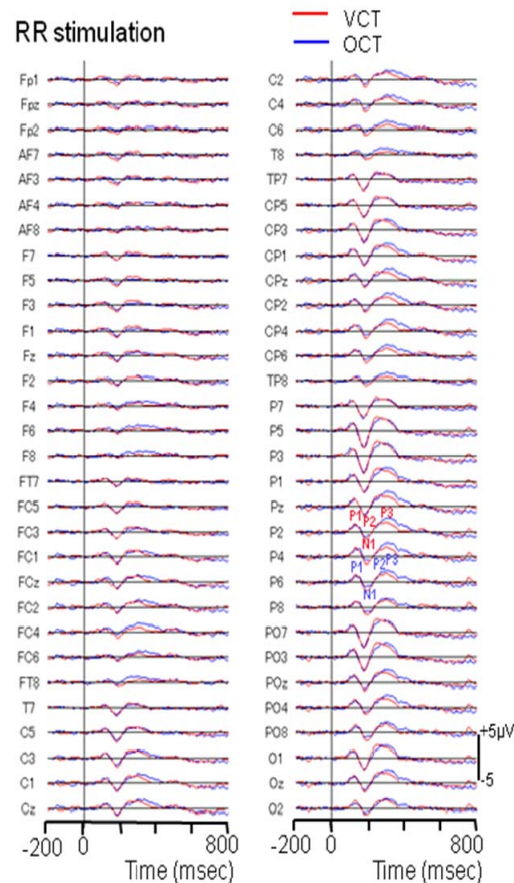
The EEG data were also analyzed by sLORETA method (Pascual-Marqui, 2002) to estimate the current source density. Briefly, sLORETA calculates the standardised current source density at each of 6239 voxels in the grey matter and the hippocampus of the MNI-reference brain. This calculation is based upon a linear weighted sum of the scalp electric potentials. sLORETA estimates the underlying sources under the assumption that neighbouring voxels should have a maximally similar electrical activity. In the present study, at each peak latency, three brain regions with the highest current source density were evaluated.

## RESULTS

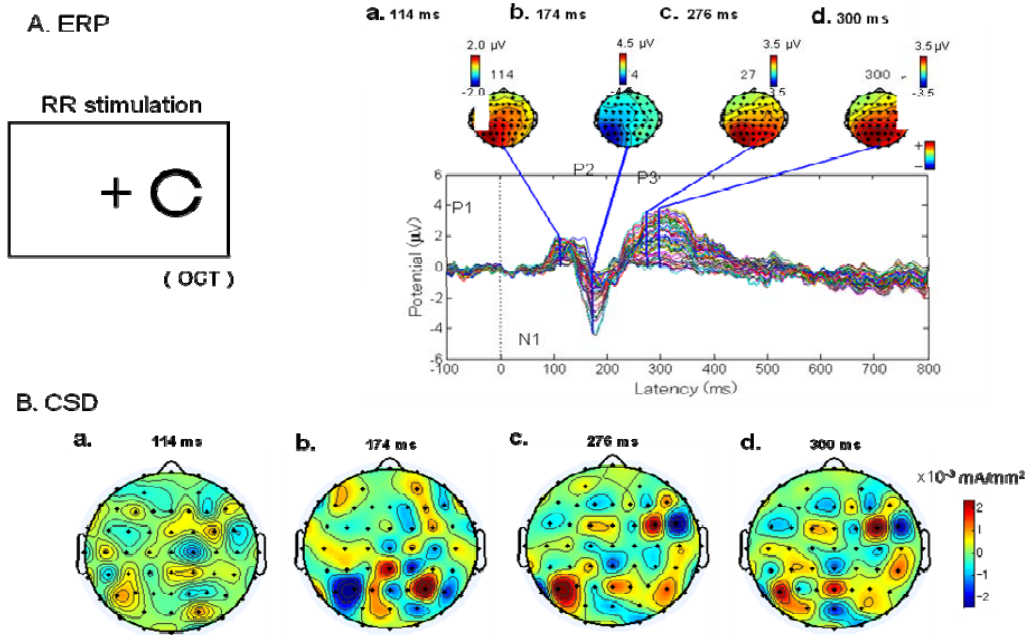
### 1) ERP wave patterns

Figure 2 shows the grand averaged ERPs when RR stimulus was presented. EEG waves were observed mainly in the parietal regions in both the VCT and OCT; 3 positive waves (P1, P2 and P3) and one negative wave (N1) were observed. Figures 3A and 4B illustrate the ERPs shown in Fig. 2 and potential topography at each peak latency. The traces of the all channels are superimposed in the figures. In the OCT (Fig. 3), EEG potentials were high in the left temporal-occipital junction at the peak latency of the positive waves (P1, P2, P3) while the EEG potentials were most negative in the same region at the peak latency of the negative wave (N1). In the CSD topography on the scalp, a weak current source was observed at the left temporal-occipital junction at peak latency of P1, and strong current sink was

observed at the left temporal-occipital junction at N1 peak latency. In addition, current sources were observed at both sides of the parietal regions. At P2 and P3 peak latencies, current source and sink were observed in the left temporal-occipital junction and right anterior frontal region. On the other hand, in the VCT using the same figure (Fig. 4), the same trend of the ERP potential topography as in the OCT was observed (A). In the CSD topography (B), current source and sink were observed in the temporal-occipital junction and the parietal region, which were similar to those in the OCT. However, unlike the OCT, current source and sink were not observed at the frontal region. These results suggest that current source generators were located in the bilateral parietal-temporal-occipital junction, and the right frontal region (especially in the OCT). In the other 3 figures, essentially similar results to those in Figs. 3 and 4 were observed.

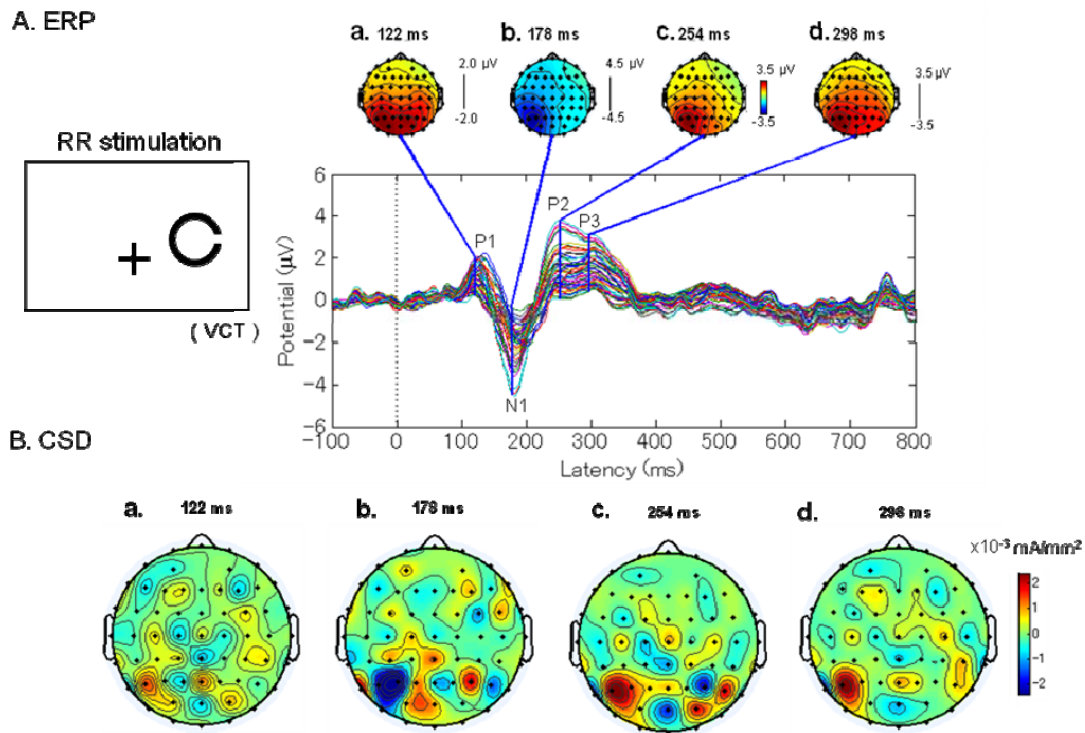


**Fig. 2.** The grand averaged ERPs in RR stimulation. In both the VCT and OCT tasks, P1, N1, P2 and P3 components were observed. Red lines, viewer-centered task (VCT); blue lines, object-centered task (OCT).



**Fig. 3.** Potential (A) and CSD (B) distribution on the scalp at the peak latencies of P1, N1, P2 and P3 components of the ERPs in the OCT task.

A: Potential topography of the ERPs shown in Fig. 2. The traces of the all channels are superimposed.  
B: CSD topography at each peak latency shown in A.



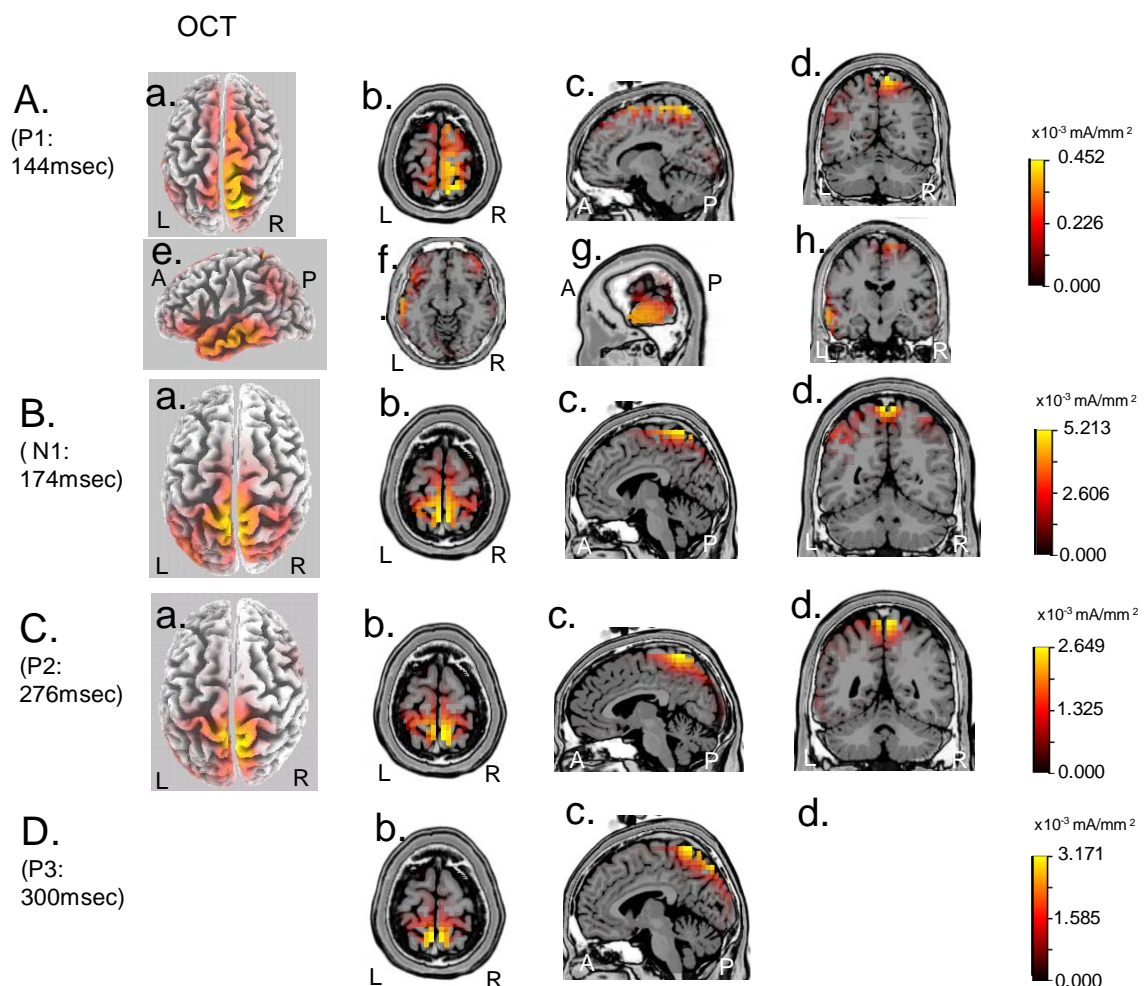
**Fig. 4.** Potential (A) and CSD (B) distribution on the scalp at the peak latencies of P1, N1, P2 and P3 components of the ERPs in the VCT task.

A: Potential topography of the ERPs shown in Fig. 2. The traces of the all channels are superimposed.  
B: CSD topography at each peak latency shown in A.

## 2) Analysis of current source density (CSD) using the sLORETA

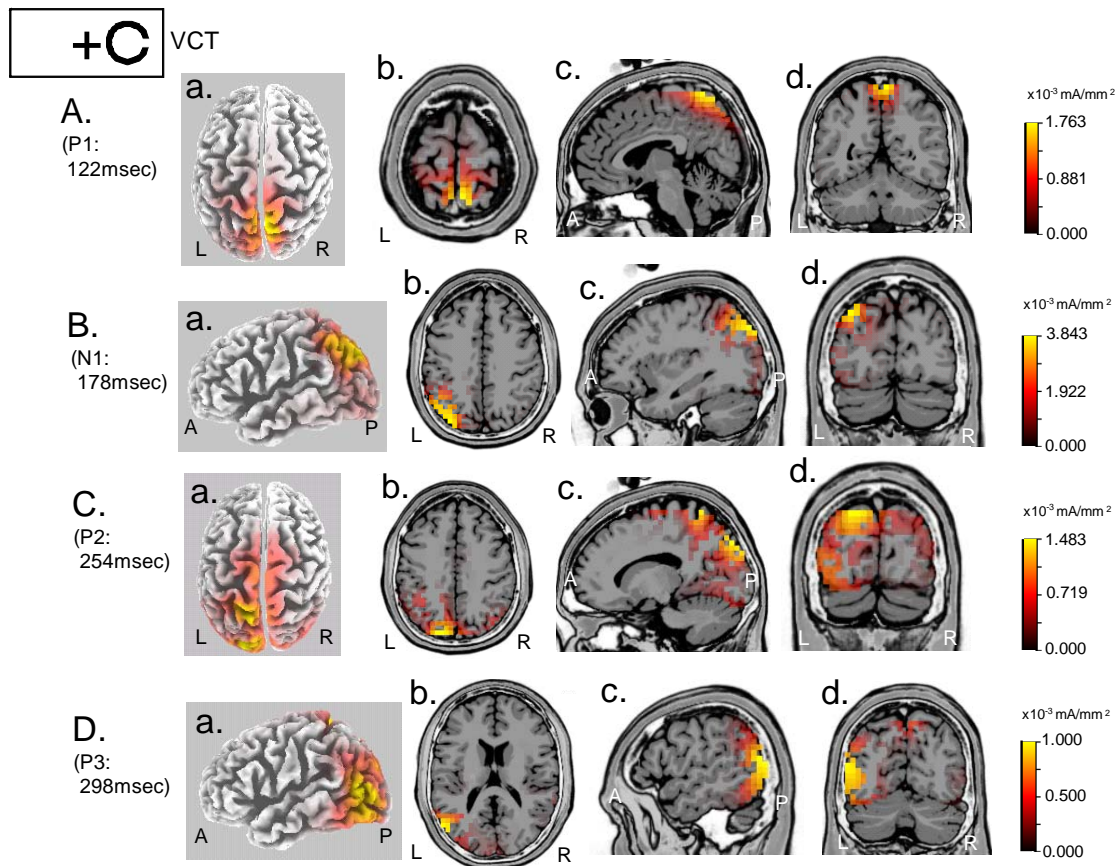
Figure 5 shows the results by sLORETA analysis of the grand averaged ERPs in the OCT where RR stimulus was presented. At P1 peak latency, current source density was high in the right superior parietal lobule, right precuneus (Aa-d) and left middle temporal gyrus (Ae-h). At N1 peak latency, current source density was high in the bilateral superior parietal lobule and left paracentral lobule (Ba-d). At P2 peak latency, current source density was high in the right paracentral lobule and right precuneus (Ca-d). At P3 peak latency, current source density was

high in the bilateral superior parietal lobule and left precuneus (Da-d). Figure 6 shows the results by sLORETA analysis of the grand averaged ERPs in the VCT where RR stimulation is used. At P1 peak latency, current source density was high in the bilateral superior parietal lobule, right paracentral lobule and right precuneus (A). At N1 peak latency, current source density was high in the left inferior parietal lobule, left precuneus, and left cuneus (B). At P2 peak latency, current source density was high in the left precuneus and left cuneus during the (C). At P3 peak latency, current source density was high in the left middle temporal gyrus (D).



**Fig. 5.** sLORETA analysis of the averaged ERPs in RR stimulation of the OCT.

A-D: Three dimensional distribution of current source density in the brain at the peak latencies of P1 (A), N1 (B), P2 (C) and P3 (D) components. The brain slices (b, axial; c, sagittal; d, frontal sections) are shown at the right side of a three dimensional images of the brain.

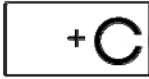

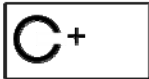
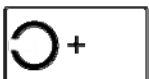


**Fig. 6.** sLORETA analysis of the averaged ERPs in RR stimulation of the VCT. Other descriptions as for Fig. 5.

Table 1 summarizes the brain regions where current source density of the ERPs was high at each peak latency of the ERP waves when each figure was presented in the OCT and VCT. The results indicated that current source density was generally high in the superior parietal lobule, inferior parietal lobule, precuneus, cuneus, superior temporal gyrus, and middle and inferior frontal gyri. Especially, in the parietal association area (superior and inferior

parietal lobule), current source density increased in all of the figures presented in both the tasks, and the right parietal association area was more active than the left side. Furthermore, comparison between the OCT and VCT indicated that activity associated with high current source density was observed in the superior frontal gyrus and superior temporal gyrus only in the OCT with RL and LR stimulation.

Table 1 Brain regions with the high current density in each ERP peak.

Figures	Object-centered task : OCT				Viewer-centered task : VCT				
	Latency(μsec)	Frontal lobe	Parietal lobe	Temporal lobe	Occipital Lobe	Latency(μsec)	Parietal lobe	Temporal lobe	Occipital Lobe
<b>RR</b> 	P1(114) N1(174) P2(278) P3(300)	R-PCL	R-SPL R-PCL RL-SPL L-PCL L-IPL R-PCun R-PCL RL-SPL L-PCun	L-MTG		P1(122) N1(178) P2(254) P3(296)	RL-SPL R-PCL R-PCun L-PCun L-IPL L-PCun	L-MTG (post.)	L-Cu L-Cu
<b>RL</b> 	P1(130) N1(188) P2(250) P3(298)	R-PCL L-SFG	RL-SPL L-IPL L-PCun L-IPL RL-SPL R-PCun RL-SPL L-PCun		L-Cu	P1(120) N1(176) P2(250) P3(268)	RL-SPL L-PCun L-IPL L-PCun L-IPL RL-SPL L-PCun RL-SPL L-PCun		L-Cu L-Cu L-Cu
<b>LR</b> 	P1(110) N1(162) P2(236) P3(258)		R-SPL R-PCun R-SPL R-PCun R-SPL R-PCun R-IPL R-SPL R-PCun R-IPL	R-STG	R-Cu	P1(116) N1(164) P2(278) P3(258)	L-PCun L-IPL R-SPL R-PCun R-IPL R-PCun R-IPL R-PCun R-IPL		L-Cu R-Cu R-Cu
<b>LL</b> 	P1(114) N1(180) P2(224) P3(262)		R-PCun R-IPL R-PCun R-IPL R-PCun R-IPL L-SPL L-PCun R-IPL		R-Cu R-Cu R-Cu	P1(118) N1(156) P2(228) P3(272)	L-SPL L-PCun L-IPL R-PCun R-IPL L-PCun RL-IPL RL-SPL L-PCun		R-Cu

SFG, Superior Frontal Gyrus; PCL, Paracentral Lobule; SPL, Superior Parietal Lobule; IPL, Inferior Parietal Lobule; PCun, Precuneus; STG, Superior Temporal Gyrus; MTG, Middle Temporal Gyrus; Cu, Cuneus.

## DISCUSSION

### 1) Neural substrates of spatial hemineglect and current source generators

The EEG potential and CSD topography indicated activity of the parietal lobe. The sLORETA analyses also indicated activity in the parietal lobe in both the VCT and OCT. In addition, sLORETA analysis, current source density was high in the superior parietal lobule, inferior parietal lobule, precuneus, cuneus, superior temporal gyrus, middle temporal gyrus and superior frontal gyrus. Consistent with the present results, these regions have been reported to be responsible for spatial neglect and to be implicated in spatial attention (Mesulam, 2000; Fink et al., 2001; Heilman and van den Abell, 1980; Shapiro et al., 2002; Young, 1992). Activity in the

right in the parietal association area (superior and inferior parietal lobule) was more frequently observed than that in the left hemisphere. Neuropsychological studies using visuospatial tasks reported that the bilateral parietal association area is involved in attention to the right visual field, while the right parietal association is involved in attention to the left visual field (Heilman and van den Abell, 1980; Weintraub and Mesulam, 1987). These findings suggest predominance of the right parietal association in spatial attention, which is also consistent with the present results.

### 2) Neural substrates of the viewer-centered and object-centered reference frames

Neggers et al. (2006) investigated the brain regions involved in the viewer-centered and

object-centered reference frames. In that study, a horizontal line and vertical line that crossed it was presented to healthy subjects, and the subjects were required to identify position of the vertical line based on the viewer-centered and object-centered reference frames. The fMRI analysis of the subjects showed that activity of the right superior parietal lobule increased when the position was identified based on the viewer-centered reference frame while activity of the right superior temporal gyrus decreased when the position was identified based on the object-centered reference frame. Hillis et al. (2005) investigated brain circulation of stroke patients using fMRI and reported that the viewer-centered neglect was associated with hypoperfusion in the posterior part of the right inferior frontal gyrus (area 44), inferior parietal lobule [supramarginal gyrus (area 40), angular gyrus (area 39)] and the cuneus (area 19), while the object-centered neglect was associated with hypoperfusion in the superior temporal gyrus (area 22) and posterior part of the inferotemporal gyrus (area 37). These results suggest that the areas associated with the viewer- and object-centered neglect correspond to the dorsal and ventral pathways for visual information processing (Mishkin and Ungerleider, 1982; Fink et al., 1997; Hillis et al., 2005; Neggers et al., 2006). The dorsal pathway is involved in information processing to identify where an object is, and the ventral pathway, in information processing to identify what an object is (Mishkin et al., 1983).

An involvement of the dorsal and ventral pathways in spatial neglect has been intensely debated; i) information of the dorsal and ventral pathways converges on the inferior parietal lobule (Young, 1992; Shapiro et al., 2002), and ii) in identification of an object location based on the viewer-centered reference frame, objects are identified in the object-centered reference frame first, and then spatial identification is performed based on that information (Foxy et al., 2003). Neurophysiological studies using monkeys reported that neurons in the supplementary eye field in the superior frontal gyrus responded to visual stimuli

based on the object-centered reference frame (Olson, 2003). These previous studies indicate that there are no consistent brain regions involved in the viewer- and object-centered reference frames. Instead, these results suggest that the 2 different systems for these 2 reference frames might overlap in the parietal association area.

In the present study, current source density was increased in the parietal lobe (superior parietal lobule and inferior parietal lobule), and right dominant activity was observed in the both OCT and VCT tasks. These results suggest that the right parietal association area is involved in the both viewer- and object-centered reference frames, consistent with the previous suggestion (Young, 1992; Shapiro et al., 2002). Furthermore, current source density was increased at the superior frontal and superior temporal gyri only in the OCT task, consistent with the previous studies (Hillis et al., 2005; Neggers et al., 2006). The results along with the previous anatomical data suggest an involvement of the dorsal visual pathways (parietal lobe) in the viewer-centered reference frame while the both dorsal (parietal lobe) and ventral (temporal lobe) visual pathways might be involved in the object-centered reference frame. These results furthermore suggest that the both visual pathways might converge on the right parietal lobe.

## REFERENCES

- Bartolomeo P, Schotten MT, Doricchi F: Left unilateral neglect as a disconnection syndrome. *Cerebral Cortex*, 17; 2479-2490, 2007.
- Bisiach E, Luzzatti C: Unilateral neglect of representational space. *Cortex*, 14: 129-133 1978.
- Bisiach E, Pizzamiglio L, Nico D, Antonucci G: Beyond unilateral neglect. *Brain*, 119: 851-857, 1996.
- Brain WR: Visual disorientation with special reference to lesions of the right cerebral hemisphere. *Brain*, 64:244 -272, 1941.

- Cals N, Devuyst G, Afsar N, Karapanayiotides T, Bogousslavsky J. Pure supratentorial posterior cerebral artery territory infarction in The Lausanne Stroke Registry. *J Neurol*, 2002; 249: 855-861.
- Chatterjee A: Picturing unilateral spatial neglect: viewer versus object-centered reference frames. *J Neurol Neurosurg Psychiatry*, 57;1236-1240, 1994.
- Delorme A, Makeig S. EEGLAB: an open source toolbox for analysis of single-trial EEG dynamics including independent component analysis. *J Neurosci Method*, 134: 9-21, 2004.
- Fink GR, Dolan RJ, Halligan PW, Marshall JC, Frith CD: Space-based and object-based visual attention: shared and specific neural domains. *Brain*, 120: 2013-2028, 1997.
- Fink GR, Marshall JC, Weiss PH, Zilles K: The neural basis of vertical and horizontal line bisection judgments: an fMRI study of normal volunteers. *Neuroimage*, 14: 559-67, 2001.
- Foxe JJ, McCourt ME, Javitt DC: Right hemisphere control of visuospatial attention: line-bisection judgments evaluated with high-density electrical mapping and source analysis. *Neuroimage*, 19; 710-726, 2003.
- Heilman KM, Bowers D, Watson RT. Performance on hemispatial pointing task by patients with neglect syndrome. *Neurology* 1983; 33: 661-664.
- Heilman KM, van den Abell T: Right hemisphere dominance for attention: the mechanism underlying hemispheric asymmetries of inattention (neglect). *Neurol*, 30; 327-330, 1980.
- Heilman KM, Valenstein E: Mechanisms underlying hemispatial neglect. *Annals of Neurology*, 5: 166-170, 1979.
- Heilman KM, Watson RT, Valenstein E: Neglect and related disorders. In *Clinical Neuropsychology*, 2nd ed, ed by Heilman KM, Valenstein E, Oxford Univ Press, New York, 1985, pp. 234-292.
- Hilgetag CC, Theoret H, Pascual-Leone A: Enhanced visual spatial attention ipsilateral to rTMS-induced 'virtual lesions' of human parietal cortex. *Nat Neurosci*, 4: 953-957, 2001.
- Hillis AE: Neurobiology of unilateral spatial neglect. *The Neuroscientist*, 12; 153-163, 2006.
- Hillis AE, Newhart M, Heidler J, Barker PB, Degaonkar M: Anatomy of spatial attention: insights from perfusion imaging and hemispatial neglect in acute stroke. *J Neurosci*, 25; 3161-3167, 2005.
- Karnath H-O, Berger MF, Küker W, Rorden C: The anatomy of spatial neglect based on voxelwise statistical analysis: a study of 140 patients. *Cerebral Cortex*, 14:1164-1172, 2004.
- Kinsbourne M: Hemi-neglect and hemisphere rivalry. *Adv Neurol*, 18: 41-49, 1977.
- Leibovitch FS, Black SE, Caldwell CB, Ebert PL, Ehrlich LE, Szalai JP: Brain-behavior correlations in hemispatial neglect using CT and SPECT: the Sunnybrook Stroke Study. *Neurology*, 50: 901-908, 1998.
- Malhotra P, Coulthard E, Husain M: Hemispatial neglect, balance and eye-movement control. *Curr Opin Neurol*, 19:14-20. 2006
- Marsh EB, Hillis AE: Dissociation between egocentric and allocentric visuospatial and tactile neglect in acute stroke. *Cortex*, 44: 1215-1220, 2008.
- Mesulam MM: A cortical network for directed attention and unilateral neglect. *Ann Neurol*, 10: 309-325, 1982.
- Mesulam MM: Spatial attention and neglect: parietal, frontal and cingulate contributions to the mental representation and attentional targeting of salient extrapersonal events. *Philos Trans R Soc Lond B Biol Sci*, 354: 1325-1346, 1999.

- Mesulam MM: Attention networks, confusional states, and neglect syndromes. In *Principles of Behavioral and Cognitive Neurology*, 2nd ed, ed by Mesulam MM, Oxford Univ Press, New York, 2000, pp. 174-256.
- Mishkin M, Ungerleider LG: Contribution of striate inputs to the visuospatial functions of parieto-preoccipital cortex in monkeys. *Behav Brain Res*, 6; 57-77, 1982.
- Mishkin M, Ungerleider LG, Macko KA: Object vision and spatial vision: two cortical pathways. *Trend in Neuroscience*, 6; 414-417, 1983.
- Myers PS: *Right Hemisphere Damage: Disorders of Communication and Cognition*. Cengage Learning: Florence, KY, 1999.
- Neggers SFW, Van der Lubbe RHJ, Ramsey NF et al: Interactions between ego-and allocentric neuronal representations of space. *Neuroimage*, 31; 320-331, 2006.
- Olson CR: Brain representation of object-centered space in monkeys and humans. *Ann Rev Neurosci*, 26; 331-354, 2003.
- Ota H, Fujii T, Suzuki K, Fukatsu R, and Yamadori A. Dissociation of body-centered and stimulus-centered representations in unilateral neglect. *Neurology*, 57: 2064–2069, 2001.
- Ota H, Fujii T, Tabuchi M, Sato K, Saito J, Yamadori A: Different spatial processing for stimulus-centered and body-centered representations. *Neurol*, 60; 1846-1848, 2003.
- Pascual-Marqui RD: Standardized low resolution brain electromagnetic tomography (sLORETA): technical details. *Methods and Findings in Experimental and Clinical Pharmacology*, 24D; 5-12, 2002.
- Shapiro K, Hillstrom AP, Husain M: Control of visuotemporal attention by inferior parietal and superior temporal cortex. *Curr Biol*, 12;1320-1325, 2002.
- Vallar G: The anatomical basis of spatial hemineglect in humans. In I. H. Robertson & J. C. Marshall (Eds.), *Unilateral neglect: Clinical and experimental studies* (pp. 27–59), 1993. Hillsdale: Lawrence Erlbaum Associates.
- Vallar G: Spatial hemineglect in humans, *Trends Cog Sci*, 2: 87–97, 1998.
- Vallar G: Extrapersonal visual unilateral spatial neglect and its neuroanatomy. *Neuroimage* 2001; 14 (1 Pt 2): S52-58.
- Vallar G, Perani D: The anatomy of unilateral neglect after right- hemisphere stroke lesions. A clinical/CT-scan correlation study in man. *Neuropsychologia* 1986; 24: 609-622.
- Weintraub S, Mesulam MM: Right cerebral dominance in spatial attention. Further evidence based on ipsilateral neglect. *Arch Neurol*, 44;621-625, 1987.
- Young MP: Objective analysis of the topological organization of the primate cortical visual system. *Nature*, 369;448-450, 1992.